DCT 250

Instrumented MSE Wall Reinforced with Polyester Straps

By

Yushan Luo
Dov Leshchinsky
Pietro Rimoldi
Giulia Lugli
Chao Xu

August, 2015

Delaware Center for Transportation
University of Delaware
355 DuPont Hall
Newark, Delaware 19716
(302) 831-1446

The Delaware Center for Transportation is a university-wide multi-disciplinary research unit reporting to the Chair of the Department of Civil and Environmental Engineering, and is co-sponsored by the University of Delaware and the Delaware Department of Transportation.

DCT Staff

Ardeshir Faghri
Director

Jerome Lewis
Associate Director

Ellen Pletz
Business Administrator I

Earl "Rusty" Lee
T^2 Program Coordinator

Matheu Carter
T^2 Engineer

Sandra Wolfe
Event Coordinator

The research reported in this document was prepared through participation in an Agreement sponsored by the State of Delaware's Department of Transportation and the Federal Highway Administration. The views and conclusions contained in this document are those of the author(s) and should not be interpreted as presenting the official policies or position, either expressed or implied, of the State of Delaware's Department of Transportation or the U.S. Federal Government unless so designated by other authorized documents.

Delaware Center for Transportation
University of Delaware
Newark, DE 19716
(302) 831-1446

Instrumented MSE Wall Reinforced with Polyester Straps

Yushan Luo[1], Dov Leshchinsky[2], Pietro Rimoldi[3], Giulia Lugli[4], and Chao Xu[5]

ABSTRACT: Mechanically Stabilized Earth (MSE) wall with large concrete panel facing, reinforced with polyester straps, is an emerging technology in the US. To enable the design of this wall system using AASHTO's methodology, its classification of extensibility must be established. Therefore, a section of such a wall was instrumented. The instrumented wall is part of a newly constructed interchange on Interstate 95 at Christiana, Delaware. It is one of several similar walls enabling an access to bridges comprising this interchange. Monitoring included tensile force distribution at selected straps and force at the connection of a few straps to the large concrete panels. The recorded data is from April, 2012, the beginning of construction of the instrumented wall, to June 2014, about 20 months after the end of its construction. When classifying this reinforced wall system as "extensible", the maximum load in the straps and connections are about 4 times smaller than predicted using AASHTO and the lengths of the reinforcing straps are adequate enabling it to mobilize the required loads. The indicated conservatism of the measured versus predicted maximum load in the reinforcements is attributed to significant underestimation of the reinforced soil strength in AASHTO's design and, potentially, to a large toe resistance. The data suggests that AASHTO's design based on extensible reinforcement for this family of MSE walls is adequate.

INTRODUCTION

Internal design of MSE walls determines the magnitude and location of the maximum load in each reinforcement layer, T_{max}. In each layer, T_{max} is a function of the frictional shear strength, ϕ, and the self-weight expressed through unit weight, γ, of the backfill soil, as well as of the surcharge loading anticipated during the life of the structure. The value of T_{max} enables the designer to select reinforcement that has adequate long-term strength. Furthermore, T_{max} is used in calculating the pullout resistive length and the required strength of the connection between the reinforcement and the facing. Clearly, T_{max} is a key value in design.

Generally, design of MSE walls in the public sector in the US is based on AASHTO. AASHTO broadly categorize reinforcement as 'extensible' (mainly geosynthetic) and 'inextensible' (mainly metallic). Although this category has a major impact on T_{max} and its location, AASHTO does not provide a tangible measure to categorize an MSE system when it comes to design. That is, categorization is purely empirical and therefore, new MSE systems

[1] PhD Student, Key Laboratory of Geotechnical and Underground Engineering of Ministry of Education, Tongji University, Shanghai, 200092, PR China and Visiting Scholar, Department of Civil and Environmental Engineering, University of Delaware, Newark, DE 19716, USA; email: luoyushan1987@gmail.com
[2] Corresponding Author. Professor Emeritus, University of Delaware and Consultant, ADAMA Engineering, PO Box 90217, Portland, OR 97290; email: dov@udel.edu
[3] Geosynthetics International Expert, Officine Maccaferri S.p.A., Corso Buenos Aires 45, Milano, Italy; email pietro.rimoldi@gmail.com
[4] Engineer, Maccaferri Inc, 10303 Governor Lane Blvd, Williamsport MD 21795, USA; email giulia.lugli@maccaferri.com
[5] Professor, Key Laboratory of Geotechnical and Underground Engineering of Ministry of Education, Tongji University, Shanghai, 200092, PR China; email: c_xu@tongji.edu.cn

have to establish their category based on field data to facilitate their acceptance in the public sector.

Fig. 1(a), reproduced from AASHTO, shows the locus of T_{max} as a function of depth below the crest, considering a wall having extensible or inextensible reinforcement. It can be seen that the loci are significantly different thus affecting the pullout resistive length which enables the reinforcement to mobilize its T_{max}. Fig. 1(b) shows the distribution of the lateral earth pressure coefficient, K_r, with depth, normalized relative to Rankine's active pressure coefficient, K_a. Note that polymer strip reinforcement is not included. The coefficient K_r is empirically-based. That is, T_{max} is calculated in design as $T_{max}= \sigma_h \cdot S_v = K_r \cdot \sigma_v \cdot S_v$ where, for a given reinforcement layer, σ_h is the average horizontal stress within the contributory vertical spacing, S_v, and σ_v is the average overburden pressure at the layer's elevation. The value of K_r was established from field measurement of T_{max} while using known S_v and σ_v to back-calculate K_r for each system category. Once the empirical K_r for a system was established, its value was divided by K_a to get a 'normalized' K_r/K_a and thus generalize its value for any permissible backfill. Note that K_a depends on ϕ and, presumably, the measured value of ϕ at the calibration test location was used to obtain K_r/K_a. Fig. 1 provides the designer with a tool which, upon broad categorization of a wall system, yields, through simple calculations, T_{max} and its location. That is, the explicit value of T_{max} and its location are obtained through calculating $K_a=\tan^2(45^o-\phi)$ based on a design value of ϕ which could be significantly different from the value used in normalizing K_r. AASHTO implicitly assumes that for a certain wall category, the normalized value K_r/K_a at a certain depth is constant for any reasonable ϕ value.

This work uses field measurements of T_{max} to categorize a wall system reinforced with polyester straps. This system has not yet been classified by AASHTO. Data was recorded during and well after the end of construction thus enabling direct assessment of K_r as well as the relative location of T_{max}. Also, the results demonstrate the inadequacy of AASHTO's normalization of K_r with respect to K_a.

INSTRUMENTED MSE WALL

General

Newly constructed complex interchange system opened to traffic in 2013, connecting I-95 and SR-1 through the arterial road SR-7, located in Christiana, New Castle County, Delaware. Due to limited space within the existing roadways and required skewed flyover alignment, 16 MSE walls, providing access to 12 bridge abutments, were constructed. The MSE walls included large precast concrete panels and high tenacity polyester straps as soil reinforcement. Since it was not known whether this wall system should be categorized as extensible or inextensible, the design was conducted twice, ultimately specifying for construction the stricter outcome. The design methodology followed LRFD as detailed in AASHTO 2007 using program MSEW(3.0). Recognizing the need to empirically categorize this wall system, Delaware Department of Transportation, DelDOT, required that one wall section (Section 4, Wall 7) be instrumented. The construction of the instrumented section was completed in October 2012 with placement of pavement, coping, and barriers done a few months later.

Reinforcement and Facing Panels

The effective height of the instrumented wall, measured from the leveling pad to the top of pavement, was 9.0 m. The uniform length of reinforcement was 8.5m with vertical spacing of

0.76m (2.5ft). Fig. 2(a) depicts the layout of the straps in the connection zone. The lower six strap layers were Maccaferri Paraweb2D/50 while the upper six layers were Maccaferri Paraweb2D/30. This proprietary reinforcing strap consists of high strength polyester filaments protected by a polyethylene coating. A section of a reinforcing strap is shown in Fig. 2(b) and relevant properties are listed in Table 1. Pullout tests conducted on straps at representative confining pressures indicate that the interaction coefficient, Ci, along the interface soil-strap was in excess of one with values higher than two for low overburden pressure. A value of Ci=0.9 was used in design to enable mobilization of the required T_{max}.

Fig. 3 shows the placement of a panel at the instrumented section, the installed panel, and the woven geotextile filter covering the joints to prevent migration of fill material. The panels, produced by Tricon Precast Limited, at the test section were 3.0 m wide by 1.5 m high by 140 mm thick. Panels had two rows of 4 loop-type connections (see Fig. 2a and 3), spaced vertically at 0.76 m.

Reinforced Backfill

Three batches of reinforced soil samples, collected at different elevations, were used for laboratory characterization. The tests were conducted at a laboratory approved by DelDOT. The summary of the reported values for sieve analyses and soil classification is presented in Table 2. For each of the three batches, three supposedly drained direct shear tests were conducted at the following normal stresses: 48, 96, and 192 kPa. Tests were conducted at a shear rate of 0.003 in/min (0.076 mm/min) on nearly saturated specimens. Table 3 provides a summary of the results obtained from the direct shear tests. In calculating the void ratios, the specific gravity of solids was assumed as 2.67.

Field compaction was specified to 95% of maximum Standard Proctor dry density. Tests conducted at the instrumented area indicate that, on average, the in-situ dry density was about γ_d=18.7 kN/m^3 (119 pcf) with a moisture content of about ω=10%. The reported values show that compaction was close to 100% Standard Proctor. Fortunately, the direct shear tests were conducted at a dry density corresponding to the actual field conditions.

For overburden stress calculations, σ_v, the average moist unit weight of the in-situ soil is $\gamma=\gamma_d(1+\omega)$=20.6 kN/m^3 (131 pcf). The Mohr-Coulomb (M-C) failure envelop intercepts at substantial cohesion values – see Table 3. This should be considered as an apparent cohesion and, per AASHTO, is ignored in design. The failure envelop for this very dense and well-graded soil should likely be curved with zero intercept; however, current design, including AASHTO's, uses M-C strength and hence, curved failure envelop is irrelevant in that context.

In a strict scientific sense, there cannot be an equivalency between M-C failure envelop with cohesion and without cohesion. That is, two lines (i.e., envelops) can intersect only at one point where the strength for a singular normal stress is identical. However, in practice there are techniques used to produce such equivalency in strength. One method, used by (*2*), relates the secant frictional strength ϕ where c=0 (i.e., the equivalent strength ϕ) to the actual M-C strength defined by c and ϕ. Their equation is $\phi_{sec}=\tan^{-1}[c/(\gamma H) + \tan\phi]$ where H for this work is the height of the wall. Substituting the reported M-C shear strength presented in Table 3 yields an equivalent strength ϕ (or ϕ_{sec} to use the notation in *2*) within a surprisingly narrow range of 49^o to 51^o; for this frictional strength the cohesion is zero. Practically, one may select a representative equivalent strength of 50^o. This 'equivalent' ϕ (for c=0) is needed for back-calculations of K_r/K_a and extensibility categorization following AASHTO methodology where cohesion is not counted for in the calibration process.

Instrumentation and Monitoring

Fig. 4 shows the layout of the load cells relevant for the objective of this study. General instrumentation included: load cells attached to the reinforcing strap (Strap Load Cell denoted as SLC in Fig. 4; photo in Fig. 5a) to yield the force in a strap at a particular location; load cells directly connected between the V-shaped strap and its attachment to the loop-connector (Facing Load Cell denoted as FLC in Fig. 4) to yield the load at the connection to the concrete panel; a 4-bar soil extensometer to indicate horizontal movement of the reinforced soil; pressure cell to measure vertical and horizontal earth pressures; and temperature sensors to evaluate its effects on the data collected. To focus on the objectives of this paper, data generated by the extensometers, pressure cells and temperature gages is not reported here; some of this data was reported by (3). Generally, the pressure cells performed poorly and unreliably. The extensometers indicated that post-construction outwards movement of the facing at mid-height was < 10 mm.

It is noted that the load cell attached to the straps (Fig. 5a) at various locations (Fig. 4) was strain gaged full-bridge attached to metal plates. The area of the plates was designed so as to produce sufficient sensitivity for reliable reading of data. The stiffness of the reduced area metal was less than half of the respective polyester strap thus increasing locally the stiffness of the strap. It is assumed that the local disturbance due to an increased stiffness has little influence on the measured loads. That is, the equivalent local stiffness of the strap and load cell, deforming in parallel, does not increase substantially to affect the behavior of reinforced system. Indeed, there is no affordable technique for precise measurement of loads in polymeric reinforcement. The two plates comprising each load cell were placed on opposite sides of the strap and clamped tightly by bolts – see Fig. 5a. The connector load cell was a commercial type, simply connected by a hook to the metal loop extending from the concrete panel. On the backfill side this load cell was connected to the strap through a customized metal loop, essentially creating a V-shaped connection of the strap as in all locations without such a load cell.

Installation and monitoring of the instrumented section started in April 2012, at the beginning of construction. Output of embedded sensors was recorded numerous times daily using a web-connected data acquisition system. Period 1 is defined until November 2, 2012, when the wall was about 8.2 m tall. Period 2 is defined between November 2, 2012 and September 13, 2013 in which construction was finished and the bridge was open to traffic for about a month. Period 3 is defined between September 13, 2013, and June 14, 2014 in which recorded data continued under normal service operating condition. Fig. 5(b), a photo taken during construction, provides an overview of the web-connected computerized data acquisition station, powered by a battery and a solar panel, some of the facing panels, the cables emerging through the facing while connected to the embedded load cells, and the outer casing of the extensometer.

MEASURED DATA

Table 4 summarizes the measured loads along straps at various locations; i.e., at elevations and distances measured from the back of the facing panels, denoted as SLC for straps and FLC for facing connection. Loads in straps at five elevations and loads at three connections were recorded – Fig. 4.

At a few locations the measured load reached a peak value shortly after construction and then followed by some relaxation. The reason for relaxation can only be speculated. It is plausible that minor soil movements occurred over time within the reinforced backfill allowing

for localized mobilization of soil strength thus reducing the need for force contribution by the strap, leading to relaxation. For the measured load at the connection, all three had substantial relaxation after the load reached a peak value. Similarly, this relaxation is probably due to a minor panels' outwards movement or tilting allowing small movement of soil near the connection and hence, dissipation of interlocking compaction stresses.

Note that the load measured in each strap is on one 'leg' or branch of its V-shaped layout (see Fig. 2a). However, analog to the pulley principle, the load per 'layer' was carried by the two branches of the same strap; i.e., by the actual reinforcement connected to the facing is considered as a layer. Hence, the measured load value on one branch has to be multiplied by 2 to quantify the total resistance generated by that layer of reinforcement. Conversely, because the two branches of each strap meet or loop at the connector load cell, the connector load cell (FLC in Fig. 4) measures directly the actual force at the connection. Consequently, half the measured load at the connections is listed in Table 4 thus making easier the comparison with the actual measured load (i.e., not twice its measured value) in the straps which is referred to as SLC – Figs. 4 and 5a.

Underlined numbers in Table 4 represent the maximum measured force and the relaxed force for the period, i.e., T_{f_max} and T_{fr_max} in that strap. The load value and corresponding location of each instrumented strap are also listed. Comparing the strap's loads at $d \approx 0$ (i.e., at the connector where half the measured connection load is listed) with the respective measured value in the same strap at d=0.6 m shows that the load at layer 8 is about the same along the front 0.6 m. However, in layer 2 the load near the connection is smaller than that at 0.6 m, whereas in layer 4 the load near the connection is somewhat larger. When conducting a field test, one would expect to obtain fluctuating data. Many factors may cause such fluctuations; e.g., non-uniform compaction, especially next to the facing; facing movement at one location more than at another; inconsistent pre-tensioning of straps as it is installed. The impact of these fluctuations on the conclusions is considered small. Finally, note that a few load cells malfunctioned after producing reliable data for some time; these cells are marked in Table 4 as "Broken".

INTERPRETATION OF MEASURED DATA

Distribution of T_{max} with Depth

AASHTO's design idealizes MSE wall problem as two dimensional (2-D), a plane strain problem. Consequently, the measured force in a strap (i.e., T_{f_max} and T_{fr_max}) needs to be translated to an equivalent force per unit length T_{max} and T_{max_r}. Note that while T_{max} is a common notation, T_{max_r} is an *ad hoc* definition and notation; it signifies the relaxed force in the equivalent 2-D reinforcement. Recall that the measured load is on one branch of the V-shaped strap. At the instrumented site, per panel width (3 m) there were four V-shaped straps connected to 4 loops at the same elevation. Therefore, considering the measured T_{f_max} and T_{fr_max}, at each elevation the load is distributed over (4×2=) 8 straps. Consequently, the equivalent 2-D load would be T_{max} or T_{max_r}, equal to T_{f_max} or T_{fr_max} each multiplied by 8 straps and divided by 3 m panel width (i.e. multiply the measured force by a factor of 8/3) resulting in force having units of kN/m, occasionally called 'knife load'.

Table 5 is a derivative of Table 4. It shows the inferred values of T_{max} and T_{max_r} (columns 4 and 7) applying a conversion factor of 8/3 on the measured force in straps. Ideally, the reinforcement force should be measured at all elevations. However, due to limited resources data was measured in 5 out of the 12 layers. It turns out that the measured T_{f_max} or T_{fr_max} versus

depth exhibits a relationship that can be grossly approximated as linear, justifying a simple interpolation of measured T_{f_max} or T_{fr_max}. Extrapolation of measured data to Layers 1, 11, and 12 can be conducted in several different ways and thus is considered speculative. Therefore, extrapolation was not performed for these three layers, as shown in Table 5. Numbers in Table 5 that are not experimental fact are clearly identified as inferred by measured data.

Note in Tables 5a and 5b that T_{max} values dropped slightly with time, perhaps implying that some soil movement developed thus mobilizing more of the soil strength and therefore, needing less contribution by the reinforcement to maintain horizontal static equilibrium. Interestingly, in Period 3 the residual and peak T_{max} values are nearly the same, perhaps implying that the wall system has reached a long term state of equilibrium.

Calculated K_r/K_a

As discussed before, it is common in design to use an empirically derived lateral earth pressure coefficient, K_r, in calculating T_{max}. AASHTO presents normalized values of K_r/K_a (Fig. 1) where K_a is Rankine's lateral earth pressure coefficient; i.e., $K_a=\tan^2(45^o - \phi/2)$. Per AASHTO, the value of K_r/K_a may vary with depth, depending on the extensibility of the system.

Using the known force in each reinforcement layer, one can conduct AASHTO's calculations in reverse. That is, AASHTO takes T_{max} and T_{max_r} as equal to $\gamma Z S_v K_r$ where γ is the moist unit weight of backfill (γ=20.6 kN/m^3), Z is the depth of the reinforcement layer from the top or the wall (i.e., Z=H-h, where H=height of the wall, 8.2 m for Period 1 and 9.0 m for Periods 2 and 3; h=height of layer from the toe -- shown in the 3rd column in Table 5) and S_v defines the tributary area of each layer (S_v= 0.76 m except for Layer 2 where it is 0.69 m). Subsequently, T_{max} and T_{max_r} should equal now to $\gamma Z S_v K_r$=20.6(H-h)$S_v K_r$. Using T_{max} and T_{max_r}, one can now assess the 'actual' K_r at each elevation. This result of such reverse-calculation ('calibration') is shown in Table 5, column 5 and 8.

Following the default value recommended by AASHTO, the designer of the wall used $\phi=34^o$ resulting in K_a= 0.283. However, in back-calculations of the normalized values of K_r/K_a, the estimated (assumed actual) soil strength of $\phi=50^o$ (Ka=0.133) was used and is presented in Table 5. Formally, if an active wedge develops, the soil should mobilize its full strength leading to an average value where $K_r \approx K_a$. The data indicates that K_r roughly varies between 0.7 and 0.9 K_a. Such a situation may happen when some of the load is carried by unaccounted elements (i.e., elements ignored in calculations) such as apparent cohesion and toe restraint. These elements contribute to redundancy in the system and are discussed in conjunction with factors of safety on the reinforcement strength.

Locus of T_{max}

The location of T_{max} at each elevation is part of the design process as it signifies the 'starting point' from which pullout resistive length is calculated – Fig. 1. As seen in Fig. 1, the locus of T_{max} is also related to extensibility.

In Fig. 6, the locus of T_{max} for extensible reinforcement is shown by a line inclined at $\theta=(45^o+\phi/2)= 70^o$ corresponding to $\phi=50^o$. Also drawn is a line at 62^o which corresponds to the value of $\phi=34^o$ commonly used in design. Table 3 and the discussion about the shear strength of backfill indicate that, effectively, ϕ could be about 50^o. The range within which the measured locus of T_{max} is wide. In fact, the location of the peak value of T_{max} along each layer seems to be insensitive (i.e., 'flat' maximum) and somewhat scattered. Hence, it cannot be used with confidence for categorization of whether the reinforcement should be treated as extensible or

inextensible. For realistic soil strength, Fig. 6 indicates that both the loci for inextensible and extensible are close to each other defining a rather shallow active zone.

Some gages ceased functioning during Period 3 (Table 5) making it difficult to identify the location of T_{max}. Therefore, in Fig. 6 only loci for Period 1 and Period 2 are shown. The best fit lines for Period 1 and Period 2 have angles of $\theta=70^o$ and $\theta=56^o$, respectively, implying ϕ to be 50^o and 22^o. However, the lack of a very distinctive location of T_{max} implies that 'predicting' ϕ based on field data while using the locus of T_{max} is unreliable. Minor changes in selecting the location of T_{max} could have θ easily change its Period 2 value from 56^o to 62^o which corresponds to $\phi=34^o$.

Variation of K_r/K_a with depth

AASHTO suggests $\phi=34^o$ as a default design value when using its recommended reinforced backfill specifications. AASHTO also limits the value of ϕ to a maximum of 40^o even if greater value is justified. This constraint is in the context of design while in back-calculations one needs to assess the actual value of soil strength.

Note that in Table 5, K_a used to normalize the inferred K_r (i.e., render K_r/K_a) is calculated based on the assessed in-situ value of $\phi=50^o$. Fig. 7 shows the variation of K_r/K_a with depth where K_a is calculated for $\phi=50^o$. Within the range of elevations where data was measured, the distribution for Period 1 in Fig. 7 is reasonably close to $K_r=K_a$, AASHTO's recommendation for extensible reinforcement (i.e., $K_r/K_a\approx1.0$).

AASHTO's normalization K_r/K_a combined with the limit $\phi\leq40^o$ could lead to inconsistent results. Assume that as implied by AASHTO's chart (Fig. 1), the ratio K_r/K_a is indeed independent of ϕ. For the sake of argument assume that this ratio was established for a case where $\phi=50^o$. Consider a case where a designer has a $\phi=50^o$ backfill; however, using AASHTO's limit of 40^o, K_a would be 0.217 for this limit rather than 0.133 for the actual backfill. Imposing the limit on ϕ to 40^o will render then T_{max} that is (0.217/0.133=) 1.63 times than actually needed. If the designer chooses to use the default value of 34^o, T_{max} would be (0.283/0.133=) 2.14 times the intended value in AASHTO's calibration. Calibrating a system based on certain parameters but then limiting the parameters in design may lead to inconsistencies. It would be wise for AASHTO to revisit its calibrated K_r/K_a in an attempt to remedy the potential inconsistency imposed by a design constraint on ϕ that may penalize the outcome significantly. Paradoxically, AASHTO's normalized calibration removes an important incentive for using high quality backfill.

Mobilized Strength of Reinforcing Straps

A direct evaluation of internal design can be done by comparing the long-term allowable strength of the reinforcement with the actual measured load. *De facto*, this ratio is the factor of safety on the reinforcement strength, usually specified in design as a minimum of Fs=1.50. The designer used reduction factors for creep considering 120 years, installation damage, and durability, equal to 1.10, 1.39, and 1.10, respectively. Hence, the long-term strength of the strap is $T_{ult}/(1.10\times1.39\times1.10)=T_{ult}/1.68$. Subsequently, one gets for peak measured load Fs $=(T_{ult}/1.68)/T_{f\_max}$ and for measured relaxed load Fs $=(T_{ult}/1.68)/T_{fr\_max}$). The calculated factors of safety, Fs, are shown in the 6th and 9th column of Table 5. Note that the straps comprising the lower layers are different from the upper layers – see Table 1. The minimum factor of safety on the long-term geosynthetic strength is 6.5 for Period 1 and 6.6 for Period 2 and Period 3. That is, the minimum actual (i.e., measured) Fs is about 4 times (6.5/1.5~6.6/1.5=4.3~4.4 times) larger than

'needed' in design. The designer followed the common practice using the default design value of $\phi=34^o$ rather than the actual $\phi=50^o$. Consistent with AASHTO calibration in Fig. 1 combined with $\phi=50^o$, this renders [$K_a(\phi=34^o)/ K_a(\phi=50^o)=0.283/0.133=$] 2.14 times larger K_r and, hence, T_{max}, than needed. Even if the designer had used the allowable upper limit of $\phi=40^o$, the outcome would have been 1.63 times larger T_{max} than needed. Subsequently, the factor of safety corrected for using reduced soil strength is about twice as calculated. Additional contributor to reduced load in the reinforcement is toe restraint. It has been demonstrated through global stability (*4*) that toe restraint can reduce the reinforcement load by as much as 50%. The instrumented wall had a 60 cm wide, well embedded, leveling pad with massive facing panels. Combining the underestimated soil strength and substantial toe restraint could reduce the load in the reinforcement by a factor of 4, quite close to the excess in actual factor of safety.

CONCLUDING REMARKS

MSE walls of significant importance were constructed in conjunction with a complex and busy interchange on I-95. The walls were comprised on large concrete facing combined with polyester straps. Such walls have not yet been categorized by AASHTO as extensible or inextensible rendering their design not fully defined. Consequently, a wall section was instrumented to ascertain the necessary design assumptions. The measured data indicates that the wall can be categorized as 'extensible' using $K_r/K_a=1.0$ at any depth.

Generally, data also indicates that the predicted loads in the reinforcement are significantly smaller when compared with design predictions. One reason is identified by the use of much smaller soil strength, $\phi=34^o$ as compared to the in-situ value of about $\phi=50^o$. This underused soil strength in design results in more than doubling the required reinforcement strength. Another likely reason for underestimation of reinforcement loads is the likely existence of high toe restraint.

While AASHTO's limitation on design value of ϕ to 40^o is sensible, it penalizes the use high quality, well-compacted backfill. That is, using AASHTO's normalized K_r/K_a while being restricted by $\phi\leq40^o$ may require the use of inflated reinforcement strength; it could be 1.5 to 2.0 stronger than needed.

ACKNOWLEDGMENTS

DelDOT required the wall producer to instrument a section of the wall to monitor the wall performance in the context of design assumptions. The authors appreciate DelDOT's progressive perspective and the subsequent funding needed for reduction and interpretation of data. The authors also thank Officine Maccaferri S.p.a. for the technical assistance in installing and web-monitoring of all instruments used in this study. The China Scholarship Council (CSC) granted to the first author, enabling her to be at UD, is greatly appreciated.

REFERENCES

American Association of State Highway and Transportation Officials (AASHTO), *LRFD bridge design specifications, 6th Edition.* Publication: LRFDUS-6-I1. Washington, DC, USA, 2012.

Miyata, Y., Bathurst, R.J., Measured and predicted loads in steel strip reinforced c-ϕ soil walls in Japan. *Soils and Foundations*, Vol. 52, No. 1, 2012, pp. 1–17.

Rimoldi, P., Leshchinsky, D., Arrigoni, M., and Bortolussi, A., Vertical wall with concrete panels facing and geostrips reinforcement: Instrumentation and Data Reduction. *Proceedings of the Design and Practice of Geosynthetic-Reinforced Soil Structures*, Bologna, Italy, 2013, pp. 243-260.

Leshchinsky, D. and Vahedifard, F., Impact of toe resistance in reinforced masonry block walls: Design dilemma. *Journal of Geotechnical and Geoenvironmental Engineering*, ASCE, Vol. 138, No. 2, 2012, pp. 236-240.

List of Tables and Figures

TABLE 1 Basic Properties of Polyester Straps Used in Instrumented Section

Designated Name	2D30	2D50
Ultimate tensile strength (T_{ult}) [kN]	30	50
Creep reduced strength (T_{cr}) [kN]	22	36
Nominal width [mm]	50	65
Nominal thickness [mm]	1.9	2.5

TABLE 2 Sieve Analysis Results on Samples Collected at Various Elevations

	Batch 1	Batch 2	Batch 3
D_{100} [mm]	4.75	4.75	4.75
D_{90}[mm]	3.20	3.30	3.60
D_{60} [mm]	0.88	0.98	1.57
D_{50}[mm]	0.45	0.49	0.99
D_{30}[mm]	0.18	0.19	0.27
D_{10}[mm]	0.05[(1)]	0.04[(1)]	0.07[(1)]
Passing #200 [%]	15.8	15.5%	11.8%
Uniformity Coef., C_u	17.6	24.5	22.4
Curvature Coef., C_c	0.74	0.92	0.66
Soil Classification	SW or A-1-b	SW or A-1-b	SW or A-1-b

[(1)]Value estimated from extrapolating gradation curve to D_{10} passing

TABLE 3 Direct Shear Tests: Data and Results

	Batch 1	Batch 2	Batch 3
Dry density,[(1)] γ_d[kN/m^3]	18.58	18.84	18.70
Moisture, [(1)]ω [%]	15.2	14.7	13.3
Void ratio, [(1)]e	0.405	0.391	0.401
[(2)]ϕ [degrees]	41.7	46.5	47.6
[(2)]c [kPa]	50.2	19.3	26.0
Disp. to peak strength, Δ[mm]	1.2 – 2.5	1.5 – 2.0	1.0 – 1.8

[(1)]Average of three tests (deviations relative to this average were insignificant)

[(2)]Shear strength parameters correspond to peak shear strength

TABLE 4 Measured Force in Reinforcing Straps

Layer # (Date)	Height from toe [m]	Distance *d* from back of facing panel [m]					
		~0.0	0.6	2.4	4.3	6.1	7.9
		Half connection load [kN]	Maximum measured force, T_{f_max}, and relaxed force, (T_{fr_max}), in strap at distance *d* from facing [kN]				
2 (11/12)	0.84	2.0 [(1)](1.3)	4.6 [(1)](3.6)	2.3	1.3	1.0 [(1)](0.8)	1.1 [(1)](1.0)
2 (09/13)	0.84	1.1 [(1)](0.6)	3.5[(1)](1.5)	3.0	1.5	1.2	1.4
2 (06/14)	0.84	0.9 [(1)](0.5)	1.7 [(1)](1.5)	3.0 [(1)](2.9)	1.7	2.2	[(2)]1.8
4 (11/12)	2.36	3.1 [(1)](2.8)	2.4 [(1)](2.2)	1.8	0.9	1.0	0.9
4 (09/13)	2.36	2.6 [(1)](1.0)	1.8 [(1)](1.0)	2.0 [(1)](0.6)	[(2)]0.7	1.3	1.6
4 (06/14)	2.36	1.2 [(1)](0.4)	1.0 [(1)](0.6)	Broken	Broken	1.3	1.7
6 (11/12)	3.88	N/A	2.0 [(1)](1.9)	2.7	1.2	1.3	1.7 [(1)](1.2)
6 (09/13)	3.88	N/A	2.0 [(1)](1.9)	3.6 [(1)](3.5)	1.5 [(1)](1.0)	1.7	[(2)]1.5
6 (06/14)	3.88	N/A	1.8	3.5	Broken	1.6	Broken
8 (11/12)	5.40	2.3 [(1)](1.5)	2.1 [(1)](1.4)	1.1	1.2	0.8	0.9
8 (09/13)	5.40	1.6 [(1)](0.8)	1.4 [(1)](0.7)	1.6	1.7	1.4	1.4
8 (06/14)	5.40	1.2 [(1)](0.5)	1.2 [(1)]0.9)	1.8	1.7	1.4 [(1)](1.3)	1.3
10 (11/12)	6.93	N/A	1.0	1.0	0.9	0.6 [(1)](0.4)	0.7
10 (09/13)	6.93	N/A	1.0	[(2)]1.2	1.4	0.6	1.2
10 (06/14)	6.93	N/A	1.1 [(1)](0.9)	Broken	1.4	0.6	1.2

[(1)]Number represents the relaxed force recorded at a point during a respective period

[(2)]The recorded load was just before the cell ceased working

TABLE 5a Measured and Inferred Data in Period 1

Layer #	Type of Strap	Height from toe, h [m]	T_{max} [kN/m]	K_r/ K_a[4] implied by T_{max}	Fs on Long-term Strength Related to T_{max}	T_{max_r} [kN/m]	K_{r_r}/ K_a[4] implied by T_{max_r}	Fs on Long-term Strength Related to T_{max_r}
1	2D/50	0.23	[3]N/A	N/A	N/A	[3]N/A	N/A	N/A
2	2D/50	0.84	12.3	0.892	6.5	9.6	0.696	8.3
3	2D/50	1.60	[2]10.4	0.752	7.6	[2]8.5	0.628	9.3
4	2D/50	2.36	[1]8.3	0.685	9.6	[1]7.5	0.619	10.6
5	2D/50	3.12	[2]7.7	0.731	10.3	[2]6.4	0.598	12.4
6	2D/50	3.88	7.2	0.805	11.0	5.1	0.570	15.7
7	2D/30	4.64	[2]6.7	0.907	7.1	[2]4.5	0.610	10.5
8	2D/30	5.40	[1]6.1	1.050	7.8	[1]4.0	0.689	11.9
9	2D/30	6.17	[2]4.5	1.045	10.5	[2]3.5	0.784	13.7
10	2D/30	6.93	2.7	1.024	17.9	2.7	1.024	17.9
11	2D/30	7.69	[3]N/A	N/A	N/A	[3]N/A	N/A	N/A
12	2D/30	8.07	[3]N/A	N/A	N/A	[3]N/A	N/A	N/A

TABLE 5b Measured and Inferred Data in Period 2

Layer #	Type of Strap	Height from toe, h [m]	T_{max} [kN/m]	K_r/K_a[4] implied by T_{max}	Fs on Long-term Strength Related to T_{max}	T_{max_r} [kN/m]	K_{r_r}/K_a[4] implied by T_{max_r}	Fs on Long-term Strength Related to T_{max_r}
1	2D/50	0.23	[3]N/A	N/A	N/A	[3]N/A	N/A	N/A
2	2D/50	0.84	9.3	0.609	8.5	4.0	0.262	19.8
3	2D/50	1.60	[2]8.1	0.534	9.6	[2]3.3	0.222	22.9
4	2D/50	2.36	[1]6.9	0.502	11.4	[1]2.7	0.196	29.8
5	2D/50	3.12	[2]8.3	0.681	9.6	[2]6.0	0.492	12.9
6	2D/50	3.88	9.6	0.905	8.3	9.3	0.875	8.5
7	2D/30	4.64	[2]7.1	0.785	6.6	[2]6.9	0.764	6.9
8	2D/30	5.40	4.5	0.602	10.5	4.5	0.602	10.5
9	2D/30	6.17	[2]4.1	0.698	11.2	[2]4.1	0.698	11.2
10	2D/30	6.93	3.7	0.862	12.8	3.7	0.862	12.8
11	2D/30	7.69	[3]N/A	N/A	N/A	[3]N/A	N/A	N/A
12	2D/30	8.07	[3]N/A	N/A	N/A	[3]N/A	N/A	N/A

TABLE 5c Measured and Inferred Data in Period 3

Layer #	Type of Strap	Height from toe, h [m]	T_{max} [kN/m]	K_r/K_a[4] implied by T_{max}	Fs on Long-term Strength Related to T_{max}	T_{max_r} [kN/m]	K_{r_r}/K_a[4] implied by T_{max_r}	Fs on Long-term Strength Related to T_{max_r}
1	2D/50	0.23	[3]N/A	N/A	N/A	[3]N/A	N/A	N/A
2	2D/50	0.84	8.0	0.524	9.9	7.7	0.504	10.3
3	2D/50	1.60	[2]6.3	0.410	12.4	[2]6.1	0.404	12.9
4	2D/50	2.36	[1]4.5	0.327	17.5	[1]4.5	0.327	17.5
5	2D/50	3.12	[2]6.9	0.566	11.4	[2]6.9	0.566	11.4
6	2D/50	3.88	9.3	0.875	8.5	9.3	0.875	8.5
7	2D/30	4.64	[2]7.1	0.785	6.6	[2]7.1	0.785	6.6
8	2D/30	5.40	4.8	0.642	9.9	4.8	0.642	9.9
9	2D/30	6.17	[2]4.3	0.732	11.2	[2]4.3	0.732	11.2
10	2D/30	6.93	3.7	0.862	12.8	3.7	0.862	12.8
11	2D/30	7.69	[3]N/A	N/A	N/A	[3]N/A	N/A	N/A
12	2D/30	8.07	[3]N/A	N/A	N/A	[3]N/A	N/A	N/A

[1]Prevailing maximum force is implied by measured connection load
[2]Values inferred by interpolation of measured values
[3]To avoid extrapolation, no data for Layers 1, 11 and 12 is inferred
[4]In 'normalizing' K_r, $K_a = tan^2(45^o - \phi/2) = tan^2(45^o - 50^o/2) = 0.133$ corresponding to $\phi = 50^o$ was used

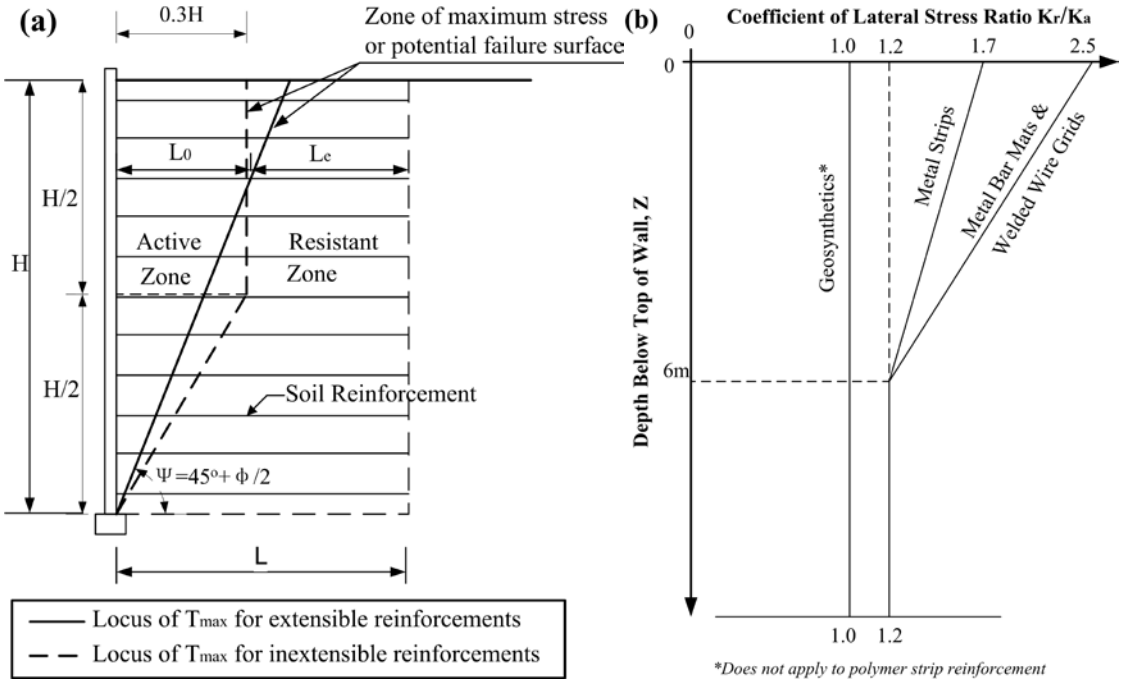

FIGURE 1 Implications of extensibility: (a) Locus of T_{max}, and (b) Variation of K_r/K_a [Reproduced from (*1*)].

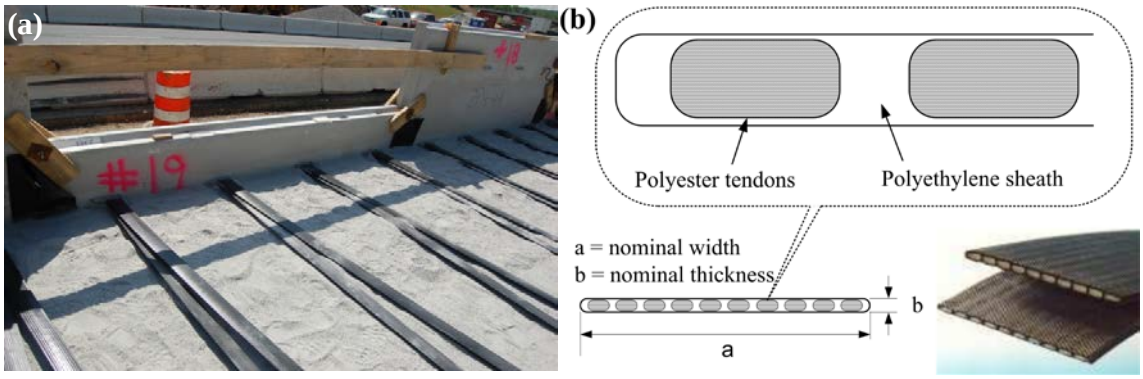

FIGURE 2 Straps: (a) Layout at the connection zone and (b) Sectional sketch.

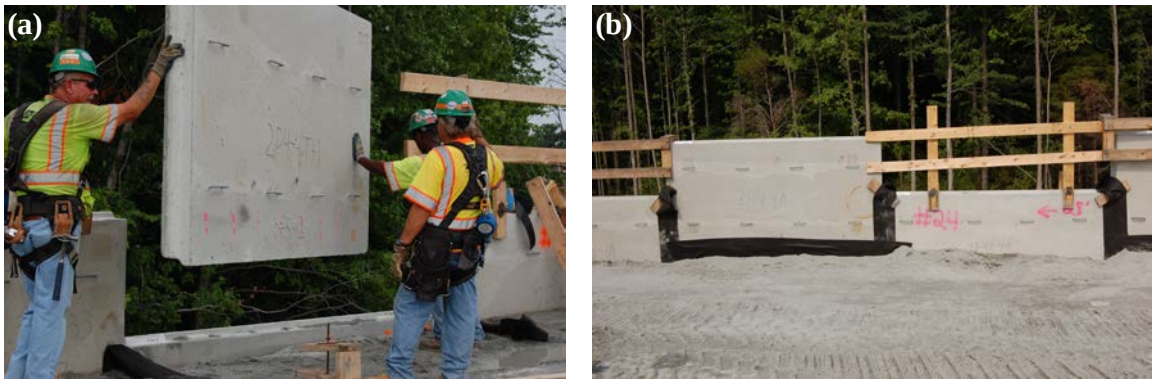

FIGURE 3 Standard precast concrete panels at the instrumented section.

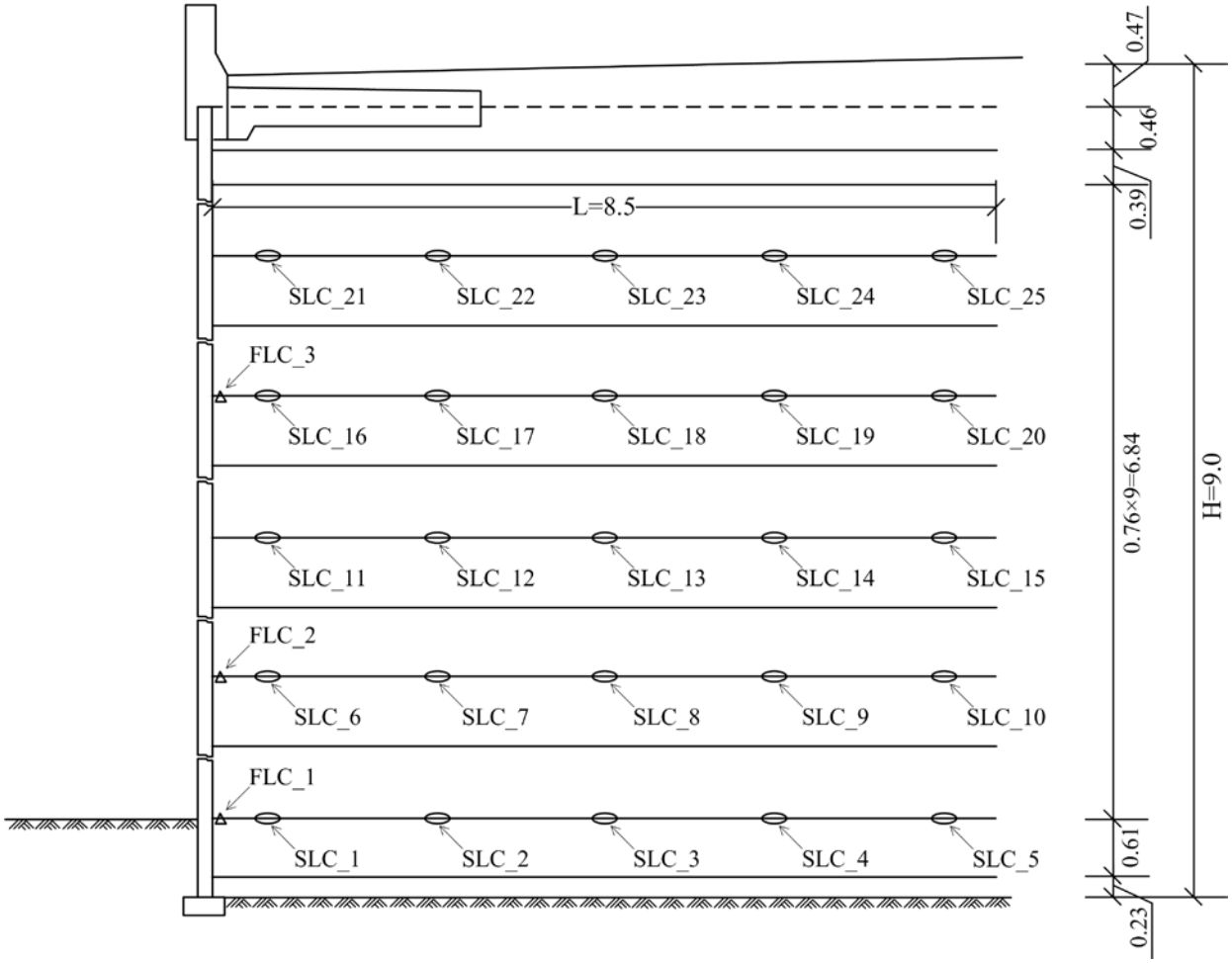

FIGURE 4 Test section: Location of sensors (all dimensions are in m).

FIGURE 5 Instrumentation: (a) Load cell attached to strap (SLC); (b) Data acquisition powered by battery charged by solar panel.

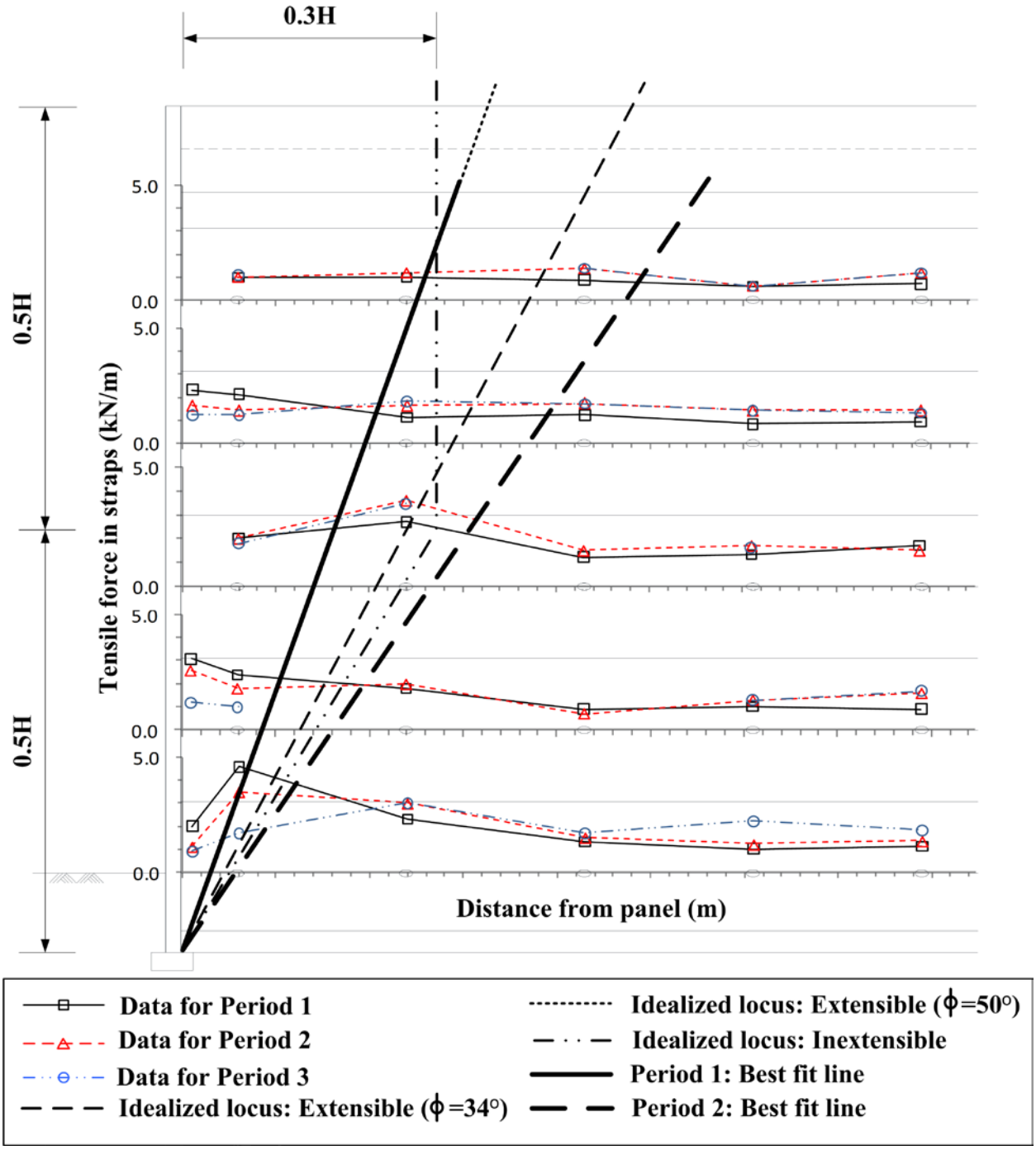

FIGURE 6 Estimated loci of T_{max} based on measured data.

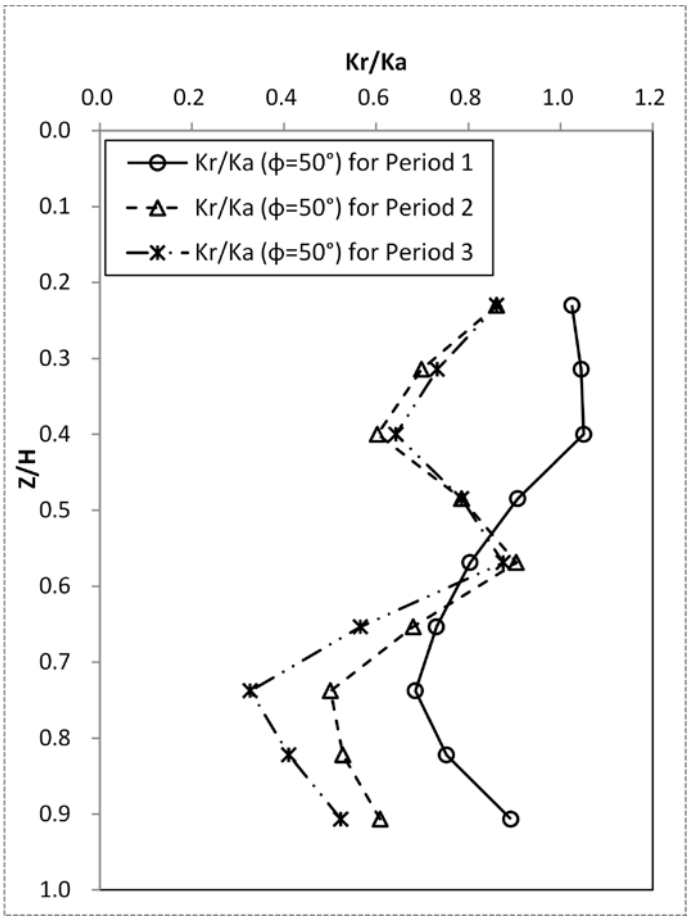

FIGURE 7 Variation of K_r/K_a with depth.

Delaware Center for Transportation University of Delaware Newark, Delaware 19716

AN EQUAL OPPORTUNITY/AFFIRMATIVE ACTION EMPLOYER

The University of Delaware does not discriminate on the basis of race, color, national origin, sex, disability, religion, age, veteran status, gender identity or expression, or sexual orientation, or any other characteristic protected by applicable law in its employment, educational programs and activities, admissions policies, and scholarship and loan programs as required by Title IX of the Educational Amendments of 1972, the Americans with Disabilities Act of 1990, Section 504 of the Rehabilitation Act of 1973, Title VII of the Civil Rights Act of 1964, and other applicable statutes and University policies. The University of Delaware also prohibits unlawful harassment including sexual harassment and sexual violence. Inquiries or complaints may be addressed to:

Susan L. Groff, Ed. D.
Director, Institutional Equity & Title IX Coordinator
305 Hullihen Hall
Newark, DE 19716
(302) 831-8063
titleixcoordinator@udel.edu

For complaints related to Section 504 of the Rehabilitation Act of 1973 and/or the Americans with Disabilities Act, please contact:

Anne L. Jannarone, M.Ed., Ed.S.
Director, Office of Disability Support Services
Alison Hall, Suite 130,
Newark, DE 19716
(302) 831-4643
OR contact the U.S. Department of Education - Office for Civil Rights (https://wdcrobcolp01.ed.gov/CFAPPS/OCR/contactus.cfm).

Abridged Version – with permission by Title IX coordinator (ex: rack cards, etc.)
The University of Delaware is an equal opportunity/affirmative action employer and Title IX institution. For the University's complete non-discrimination statement, please visit www.udel.edu/aboutus/legalnotices.html